Available online at www.sciencedirect.com

ScienceDirect

IFAC Papers Online CONFERENCE PAPER ARCHIVE

IFAC-PapersOnLine 49-21 (2016) 501–506

A Global Optimal Control Methodology and its Application to a Mobile Robot Model

E. Dincmen

Işık University, 34980, Şile, İstanbul, Turkey
(Tel: 0090-2165287127; e-mail: erkin.dincmen@isikun.edu.tr).

Abstract: A global optimal control algorithm is developed and applied to an omni-directional mobile robot model. The aim is to search and find the most intense signal source among other signal sources in the operation region of the robot. In other words, the control problem is to find the global extremum point when there are local extremas. The locations of the signal sources are unknown and it is assumed that the signal magnitudes are maximum at the sources and their magnitudes are decreasing away from the sources. The distribution characteristics of the signals are unknown, i.e. the gradients of the signal distribution functions are unknown. The control algorithm also doesn't need any position measurement of the robot itself. Only the signal magnitude should be measured via a sensor mounted on the robot. The simulation study shows the performance of the controller.

Keywords: Global optimization, mobile robot, extremum seeking.

1. INTRODUCTION

When a mobile robot operates in an unknown terrain with no GPS signal and no inertial measurements, it should use an extremum seeking algorithm to search and find the target point such as a signal source. Various types of extremum seeking algorithms are developed in the literature. In the perturbation based extremum seeking algorithms (Ghaffari et al., 2014; Krstic and Wang, 2000; Zhang et al., 2007) disturb and observe methods are studied by adding a perturbation to the search signal. According to the effect on the system output, the search signal is increased or decreased. In sliding mode based technique (Dincmen et al., 2014; Dincmen and Guvenc, 2012; Drakunov et al., 1995; Fu and Ozguner, 2011; Haskara et al., 2000), a sliding surface is selected such that when the system is in sliding mode, the states move towards the a priori unknown optimum operation point. The numerical optimization based schemes (Vweza et al., 2015; Zhang and Ordonez, 2007) use various iteration algorithms to find the optimum operation point. The iteration method finds the target state and a state regulator manage the system follow this new state. In the fourth group of extremum seeking methods (Guay and Dochain, 2015; Guay, 2014), the search procedure is accomplished via adaptive gradient estimation techniques.

In this paper, a new sliding mode based extremum seeking algorithm is developed where the sliding mode technique is utilized to estimate the gradient of the unknown signal distribution function. In that way, the proposed methodology embodies the characteristics of the second and fourth extremum seeking algorithms presented above. The algorithm is applied to an omni-directional mobile robot signal source seeking problem. Omni-directional mobile robots (Barreto et al., 2014; Kim and Kim, 2014; Li et al., 2015) are holonomic robots which have wheels with free rollers.

When there are multiple signal sources in the operation region of the mobile robot, and if the aim is to find the most intense signal source among the other sources, then this is a global optimization problem. The control algorithm developed in this paper will seek the global maximum point when there are local extremas. It doesn't need to know the signal distribution characteristics, the locations of the signal sources and position of the robot itself. Henceforth, it can be used in the missions where the robot moves in an unknown terrain with no GPS and no inertial measurements. Only the magnitude of the signal should be measured via a sensor mounted on the robot itself.

The rest of the paper is organized as follows: In Section 2, the control algorithm is introduced. Mobile robot model is given in Section 3. Simulation study in Section 4 shows the performance of the control algorithm. The paper ends with conclusions in Section 5

2. CONTROL ALGORITHM

Change of the signal value with respect to the inertial coordinates x,y is denoted here as a nonlinear performance function $J(x,y)$. The controller doesn't know this function i.e. the gradients of the function and its extremum points are unknown. Only its magnitude can be measured via a sensor on the robot. The aim is to find the global extremum point of $J(x,y)$.

2.1 Gradient Estimation Algorithm

For the gradient estimator, a sliding surface variable s is defined as

$$s = J(x,y) + z_1 + z_2 \,, \tag{1}$$

where the time derivatives of the variables z_1 and z_2 are defined as $\dot{z}_1 = -\dot{x}u_1$ and $\dot{z}_2 = -\dot{y}u_2$. Here, u_1 and u_2 are

10.1016/j.ifacol.2016.10.652

discontinuous functions of s and they will be defined later. The time derivative of (1) can be written as

$$\dot{s} = \frac{\partial J}{\partial x}\dot{x} + \frac{\partial J}{\partial y}\dot{y} - \dot{x}u_1 - \dot{y}u_2 . \quad (2)$$

Now, for some time interval Δt_1, when only the motion on x axis is allowed, then, since $\dot{y} = 0$ during this interval, the equation given in (2) becomes

$$\dot{s} = \frac{\partial J}{\partial x}\dot{x} - \dot{x}u_1 . \quad (3)$$

Since the motion is maintained on x axis during Δt_1, then $\dot{x} \neq 0$ will be true in (3). By remembering that u_1 is a discontinuous function of s, then, when $\dot{s} = 0$ is accomplished, from (3), the equivalent value of the discontinuous function u_1 will be equal to

$$u_{1eq} = \left(\frac{\partial J}{\partial x}\right)_{est} . \quad (4)$$

In other words, estimation of the gradient with respect to x will be accomplished by calculating the equivalent value of the discontinuous function u_1. To obtain the equivalent value of u_1, a low-pass filter can be used as

$$\left(\frac{\partial J}{\partial x}\right)_{est} = u_{1eq} = \frac{1}{\tau_1 p + 1}u_1 , \quad (5)$$

where τ_1 is the filter time constant and p is the complex variable of the Laplace transform. So, in (5), $1/(\tau_1 p + 1)$ is the transfer function of a first order system, which is the low-pass filter here. The rationale using a low-pass filter to obtain the equivalent value of the discontinuous function u_1 can be explained as follows: Since u_1 is a discontinuous function of s, during sliding mode, i.e. when $\dot{s} = 0$, it will oscillate with high frequency. The mean value (equivalent value) of these oscillations can be derived by filtering out the high frequency component by using a low-pass filter.

For another time interval Δt_2, when only motion on y axis is allowed, then, since $\dot{x} = 0$ during this interval, the equation given in (2) becomes

$$\dot{s} = \frac{\partial J}{\partial y}\dot{y} - \dot{y}u_2 . \quad (6)$$

Again, since during Δt_2 the motion on y axis is maintained, it is true that $\dot{y} \neq 0$. If $\dot{s} = 0$ is accomplished in (6), then the equivalent value of the discontinuous function u_2 will be equal to

$$u_{2eq} = \left(\frac{\partial J}{\partial y}\right)_{est} , \quad (7)$$

which is the estimate of the gradient with respect to y. To obtain the equivalent value of the discontinuous function u_2, a low pass filter similar to (5) can be used as

$$\left(\frac{\partial J}{\partial y}\right)_{est} = u_{2eq} = \frac{1}{\tau_2 p + 1}u_2 . \quad (8)$$

So, the gradients of the performance function with respect to x and y can be estimated as u_{1eq} and u_{2eq}. It should be reminded that the shape of the performance function $J(x,y)$ is unknown. Henceforth, the exact gradient values $\partial J/\partial x$ and $\partial J/\partial y$ are unknown. The controller will use only the estimated values of the gradients, which are u_{1eq} and u_{2eq} calculated from (5) and (8).

2.2 Gradient Climbing Rule

Desired velocity values on x and y axes can be calculated by using the estimated gradient values according to the gradient climbing rules of

$$\dot{x}_{set} = V_1 \,\mathrm{sgn}^*\left(\frac{\partial J}{\partial x}\right)_{est} = V_1 \,\mathrm{sgn}^*(u_{1eq}) , \quad (9)$$

$$\dot{y}_{set} = V_2 \,\mathrm{sgn}^*\left(\frac{\partial J}{\partial y}\right)_{est} = V_2 \,\mathrm{sgn}^*(u_{2eq}) , \quad (10)$$

where V_1 and V_2 are positive constants and representing the step sizes of the motion during gradient climbing. The function sgn* is defined as

$$sgn^*(\varepsilon) = \begin{cases} 1 & \text{if } \varepsilon \geq 0 \\ -1 & \text{otherwise} \end{cases} . \quad (11)$$

According to (9), (10) and (11), the reference velocities take values of $\dot{x}_{set} = \pm V_1$ and $\dot{y}_{set} = \pm V_2$. The equivalent values of the discontinuous functions u_1 and u_2 are the estimated gradients as in (4) and (7). The gradient estimation will be valid if $\dot{s} = 0$ in (3) and (6). The necessary conditions for accomplishing $\dot{s} = 0$ are given in the following subsection.

2.3 Necessary Conditions to Make $\dot{s} = 0$

For the interval of Δt_1, where the motion is only on x axis, the sliding surface dynamics was given in (3). Here, if the discontinuous function u_1 is selected as

$$u_1 = M_1 \,\mathrm{sgn}\left[\sin\left(\frac{\pi s}{\gamma_1}\right)\right], \quad (12)$$

where M_1 and γ_1 are positive constants, "sgn" is the signum function and "sin" is the sinusoidal function, then, if M_1 is chosen to satisfy the condition

$$M_1 > \left|\frac{\partial J}{\partial x}\right|_{\max} , \quad (13)$$

then after a finite time interval, $\dot{s} = 0$ will be accomplished.

Proof: By integrating (3) with (12), one can obtain

$$\dot{s} = \frac{\partial J}{\partial x}\dot{x} - \dot{x}M_1 \,\mathrm{sgn}\left[\sin\left(\frac{\pi s}{\gamma_1}\right)\right]. \quad (14)$$

By assuming perfect velocity set point tracking, from (9) one can write $\dot{x} = \dot{x}_{set} = \pm V_1$. When $\dot{x} = V_1$, (14) can be written as

$$\dot{s} = \frac{\partial J}{\partial x}V_1 - V_1 M_1 \,\mathrm{sgn}\left[\sin\left(\frac{\pi s}{\gamma_1}\right)\right]. \quad (15)$$

If the initial value of s is between values $\gamma_1 < s(0) < 2\gamma_1$, then the following mathematical equality can be written on that interval

$$\operatorname{sgn}\left[\sin\left(\frac{\pi s}{\gamma_1}\right)\right] = \operatorname{sgn}(s - 2\gamma_1). \tag{16}$$

For example if $s = 3\gamma_1/2$, then both sides of the above equation will be -1. By using (16), (15) becomes

$$\dot{s} = \frac{\partial J}{\partial x} V_1 - V_1 M_1 \operatorname{sgn}(s - 2\gamma_1). \tag{17}$$

If a variable λ is defined as $\lambda = s - 2\gamma_1$, since $\dot{\lambda} = \dot{s}$, one can write

$$\dot{\lambda} = \frac{\partial J}{\partial x} V_1 - V_1 M_1 \operatorname{sgn}(\lambda). \tag{18}$$

By multiplying (18) with λ, one can obtain

$$\lambda\dot{\lambda} = \frac{\partial J}{\partial x} V_1 \lambda - V_1 M_1 |\lambda|. \tag{19}$$

From (19), the following inequality can be written

$$\lambda\dot{\lambda} \le \left|\frac{\partial J}{\partial x}\right| V_1 |\lambda| - V_1 M_1 |\lambda| = -V_1 |\lambda| \left(M_1 - \left|\frac{\partial J}{\partial x}\right| \right). \tag{20}$$

So, when M_1 is chosen to satisfy the condition (13), the absolute value of λ will decrease and approach to zero in finite time. After the finite time interval, $\lambda = 0$ and since $\lambda = s - 2\gamma_1$, the sliding variable s will be equal to the constant value $s = 2\gamma_1$ resulting that $\dot{s} = 0$. It should be noted that the condition (13) means that the value of M_1 should be selected larger than the maximum value of the gradient with respect to x. Although the gradient is unknown since signal distribution function is unknown, still one can anticipate the maximum possible gradient value and choose an M_1 value which will always satisfy the condition (13).

The above analysis was conducted when $\dot{x} = V_1$. Now, by assuming that $\dot{x} = -V_1$, then (14) can be written as

$$\dot{s} = -\frac{\partial J}{\partial x} V_1 + V_1 M_1 \operatorname{sgn}\left[\sin\left(\frac{\pi s}{\gamma_1}\right)\right]. \tag{21}$$

Again, if the initial value of s is between $\gamma_1 < s(0) < 2\gamma_1$, the following mathematical equality can be also written on that interval

$$\operatorname{sgn}\left[\sin\left(\frac{\pi s}{\gamma_1}\right)\right] = -\operatorname{sgn}(s - \gamma_1). \tag{22}$$

So, (21) becomes

$$\dot{s} = -\frac{\partial J}{\partial x} V_1 - V_1 M_1 \operatorname{sgn}(s - \gamma_1). \tag{23}$$

This time, if the variable λ is defined as $\lambda = s - \gamma_1$, since $\dot{\lambda} = \dot{s}$, one can write

$$\dot{\lambda} = -\frac{\partial J}{\partial x} V_1 - V_1 M_1 \operatorname{sgn}(\lambda). \tag{24}$$

By multiplying (24) with λ, one obtains

$$\lambda\dot{\lambda} = -\frac{\partial J}{\partial x} V_1 \lambda - V_1 M_1 |\lambda|. \tag{25}$$

From (25), one can write

$$\lambda\dot{\lambda} \le \left|\frac{\partial J}{\partial x}\right| V_1 |\lambda| - V_1 M_1 |\lambda| = -V_1 |\lambda| \left(M_1 - \left|\frac{\partial J}{\partial x}\right| \right). \tag{26}$$

Equation (26) means that by choosing M_1 satisfying the condition (13), the absolute value of λ will decrease and after a finite time interval, $\lambda = 0$ and since $\lambda = s - \gamma_1$, the sliding variable s will be equal to the constant value $s = \gamma_1$ resulting that $\dot{s} = 0$. The above analysis can be conducted not only for $\gamma_1 < s(0) < 2\gamma_1$ but for any initial value of $s(0)$. So, whatever the initial value of s is, after a finite time interval, s will equal to a constant value and hence $\dot{s} = 0$ will be accomplished. *End of proof*

Above proof shows that during motion on x axis, $\dot{s} = 0$ can be accomplished, and hence the gradient with respect to x can be estimated via (5). Same analysis can be conducted during motion on y axis. It can be shown that during the time interval of Δt_2, when only the motion on y axis is allowed, by choosing the function u_2 as

$$u_2 = M_2 \operatorname{sgn}\left[\sin\left(\frac{\pi s}{\gamma_2}\right)\right], \tag{27}$$

where M_2 and γ_2 are positive constants, and when M_2 is selected to satisfy the inequality

$$M_2 > \left|\frac{\partial J}{\partial y}\right|_{\max}, \tag{28}$$

then, after a finite time, $\dot{s} = 0$ is accomplished and the gradient with respect to y can be estimated via (8).

2.4 Searching the Global Extremum Point

When there are local extremas in the operation region, the mobile robot will stuck in one of them. To continue the search for global extremum, the robot should leave the local extremum point. In order to accomplish this, two different operation modes are defined. In the "gradient climbing mode", the mobile robot will move on x and y axes in sequence according to the gradient climbing rules given in (9) and (10). Note that this paper doesn't include a velocity controller. It is assumed that the mobile robot can track the reference velocities calculated from (9) and (10) perfectly. For a velocity controller, a well known PID controller can be used. During the "gradient climbing mode", robot approaches towards the extremum point by performing a stair shaped trajectory as shown in Fig. 6. When the extremum point is reached, "gradient climbing mode" is deactivated and "single move mode" will be active. In this second mode, the robot will move away from the extremum point and step into a neighborhood. Then, "gradient climbing mode" will be

activated again to initiate a new search towards the extremum point. The shape of the performance function and the location of the extremum points are unknown. However, the number of extremum points, i.e. the number of signal sources should be known in advance in order the robot not to continue its search forever. Once each extremum point has been found, the robot will compare the signal magnitude levels on each visited extremum points. Without any GPS signal and inertial measurements, the robot can move towards the global extremum point by repeating backwards its motion history. The graphical representation of the global search algorithm is shown in Fig. 1. The block diagram of the robot modes are given in Fig. 2. Switch block in Fig. 2 changes the operation modes. When the robot reaches an extremum point, e.g. region 2 in Fig. 1, the change of the signal level will be very small, hence the switch will activate the single move mode. In this mode, the robot will move linearly for a predefined amount of time in order to leave the extremum point and start a new search. Flow diagram of the robot operation is shown in Fig. 3.

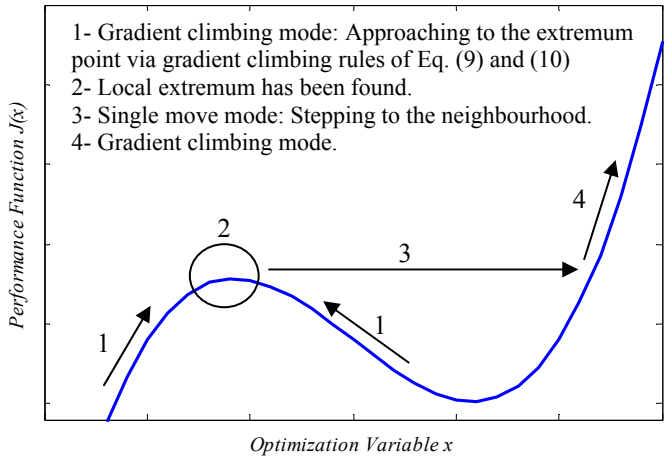

Fig. 1. Schematic representation of the global extremum seeking.

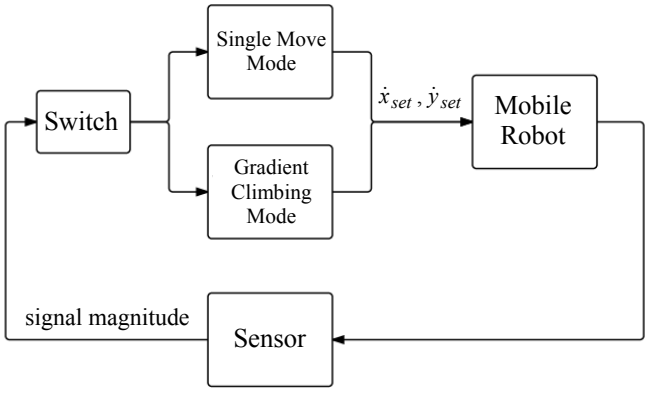

Fig. 2. Operation modes.

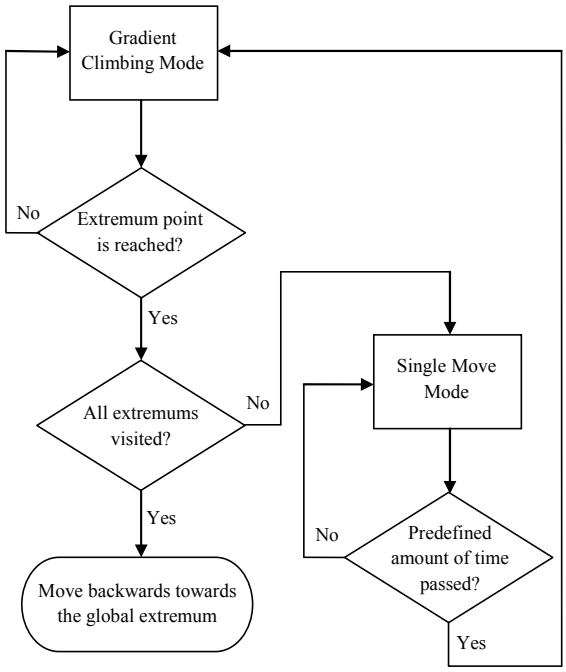

Fig. 3. Flow diagram.

3. MOBILE ROBOT MODEL

Here, a three-wheeled omni-directional mobile robot model is considered. Each wheel has free rollers that results a holonomic mobile robot. In Fig. 4, the robot model is shown. V_{w1}, V_{w2} and V_{w3} are the translational velocities of the wheels. The velocity of the robot on its longitudinal axis is denoted as u, the velocity on its lateral axis is denoted as v and r is the rotational velocity of the robot around its center. The rotational angle of the robot is denoted as θ. Robot radius is denoted as R and α is the angular position of the second wheel with respect to the longitudinal axis of the robot. Third wheel is located symmetrical to the second wheel.

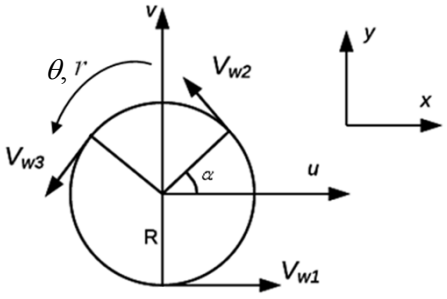

Fig. 4. Three wheeled omni-directional mobile robot model.

The velocity relationships between the inertial frame and robot moving frame is written as

$$\begin{bmatrix}\dot{x}\\ \dot{y}\\ \dot{\theta}\end{bmatrix}=\begin{bmatrix}cos(\theta) & -sin(\theta) & 0\\ sin(\theta) & cos(\theta) & 0\\ 0 & 0 & 1\end{bmatrix}\begin{bmatrix}u\\ v\\ r\end{bmatrix}. \quad (29)$$

It is assumed that there is no slip in the tangential direction at the mobile robot wheels. Then, the translational velocities of the wheels can be calculated from the rotational velocities as $V_{wi}=R_w\omega_i$, (i=1,2,3) where R_w is the wheel radius and ω_i are the angular velocities of the wheels. The velocity relationships between the wheel angular velocities and robot translational and rotational velocities is written as

$$\begin{bmatrix}\omega_1\\ \omega_2\\ \omega_3\end{bmatrix}=\frac{1}{R_w}\begin{bmatrix}1 & 0 & R\\ -\sin(\alpha) & \cos(\alpha) & R\\ -\sin(\alpha) & -\cos(\alpha) & R\end{bmatrix}\begin{bmatrix}u\\ v\\ r\end{bmatrix}. \quad (30)$$

In this paper, it is considered that the mobile robot doesn't rotate around its axis i.e., $\theta = 0$ and $r = 0$. Then, from (29) one can write $\dot{x}=u$ and $\dot{y}=v$. From longitudinal and lateral set-point velocities calculated in (9) and (10), and via the help of kinematic equation (30), the desired wheel angular velocities can be calculated as in (31).

$$\begin{bmatrix}\omega_{1set}\\ \omega_{2set}\\ \omega_{3set}\end{bmatrix}=\frac{1}{R_w}\begin{bmatrix}1 & 0 & R\\ -sin(\alpha) & cos(\alpha) & R\\ -sin(\alpha) & -cos(\alpha) & R\end{bmatrix}\begin{bmatrix}\dot{x}_{set}\\ \dot{y}_{set}\\ 0\end{bmatrix}. \quad (31)$$

A PID controller can be used for the wheel motors to track the reference velocities calculated from (31). This paper doesn't propose a velocity controller and perfect velocity tracking is assumed.

4. SIMULATION STUDY

The signal distribution characteristic is simulated here via the following performance function (Matveev et al., 2011),

$$J(x,y)=10e^{-\frac{(x-10)^2+(y-8)^2}{600}}+18e^{-\frac{(x+20)^2+(y+12)^2}{200}}. \quad (32)$$

It should be reminded that the controller doesn't know the function (32). It only knows the magnitude of the signal via a sensor on the mobile robot. The plot of the performance function (32) is shown in Fig. 5. The signal distribution function has two extremum values. In Fig. 6, the robot trajectory during the simulation is shown. The initial point of the robot was chosen as $x(0)$=3, $y(0)$=3. Firstly, it moved towards the local extremum point of the region via the gradient climbing rules (9) and (10). Once the extremum point was found, the robot moved linearly for a predefined amount of time in order to reach to a different region. Then, again via the gradient climbing rule, it reached the extremum point of the region. Since the last extremum point is the global extremum, control algorithm stopped and the robot remained on this point. It should be noted that although the gradient climbing rules (9) and (10) includes sgn terms, their values will oscillate only when the robot reaches to an extremum point because the gradient changes its sign around the extremum point. This will cause no problem because once the robot reaches an extremum point, it will leave this point and begin a new search.

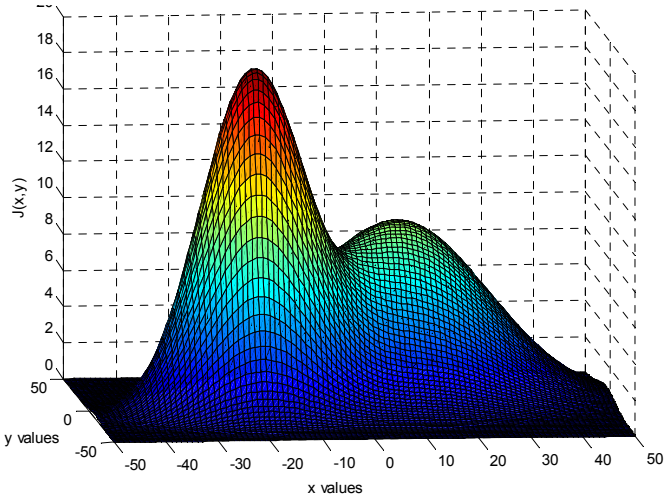

Fig. 5. Signal distribution function (32).

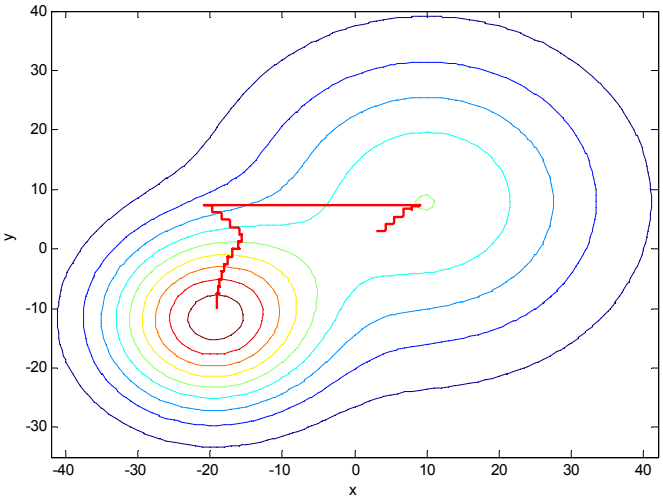

Fig. 6. Trajectory of the robot.

5. CONCLUSION

A global extremum seeking algorithm is introduced and applied to the signal source seeking problem of a mobile robot model. Without knowing the signal distribution function and the location of the extremum points, and without using a GPS signal and inertial measurements, the robot can find the global extremum point i.e. the most intense signal source among the other local extremas. Hence, the developed controller is suitable for robots operating in unknown terrains with no GPS and inertial measurements. Only the signal magnitude should be measured via a sensor mounted on the robot. The simulation study shows that the robot can find the global extremum point. In the gradient climbing mode, the motion of the robot is determined via the estimation of the gradients as in (9) and (10). Since the sign of the gradient changes only around the peak points, the control input will oscillate only around the extremum points. This will cause no problem because once the robot reaches an extremum point, it will leave this point and begin a new search. Finally, after visiting all extremas, the robot will move towards the global extremum point by repeating its motion history backwards.

REFERENCES

Barreto, C. L., Conceicao, A. G. S., Dorea, C.E.T., Martinez, L., Roberto de Pieri, E. (2014). Design and implementation of model-predictive control with friction compensation on an omnidirectional mobile robot. *IEEE/ASME Transactions on Mechatronics*, 19 (2), 467-476.

Dincmen, E., Guvenc, B.A., Acarman, T. (2014), Extremum seeking control of ABS braking in road vehicles with lateral force improvement. *IEEE Transactions on Control Systems Technology*, 22 (1), 230-237.

Dincmen, E., Guvenc, B. A. (2012). A control strategy for parallel hybrid electric vehicles based on extremum seeking. *Vehicle System Dynamics*, 50 (2), 199-227.

Drakunov, S., Özgüner, Ü., Dix, P., Ashrafi, B. (1995). ABS control using optimum search via sliding modes. *IEEE Transactions on Control Systems Technology*, 3 (1), 79–85.

Fu, L., Özgüner, Ü. (2011). Extremum seeking with sliding mode gradient estimation and asymptotic regulation for a class of nonlinear systems. *Automatica*, 47, 2595-2603.

Ghaffari, A., Krstic, M., Seshagiri, S. (2014). Power optimization and control in wind energy conversion systems using extremum seeking. *IEEE Transactions on Control Systems Technology*, 22 (5), 684-1695.

Guay, M., Dochain, D. (2015). A multi-objective extremum-seeking controller design technique. *International Journal of Control*, 88 (1), 38-53.

Guay, M. (2014). A time-varying extremum-seeking control approach for discrete-time systems. *Journal of Process Control*, 24 (3), 98-112.

Haskara, I., Ozguner, U., Winkelman, J. (2000). Extremum control for optimal operating point determination and set point optimization via sliding modes. *Journal of Dynamic Systems, Measurement, and Control*, 122 (4), 719-724.

Kim, H., Kim, B.K. (2014). Online minimum-energy trajectory planning and control on a straight-line path for three-wheeled omnidirectional mobile robots. *IEEE Transactions on Industrial Electronics*, 61 (9), 4771-4779.

Krstic, M., Wang, H.H. (2000). Stability of extremum seeking feedback for general nonlinear dynamic systems. *Automatica*, 36 (4), 595-601.

Li, X., Zhao, G., Jia, S., Xu, C., Qin, B. (2015). Velocity measurement for omni-directional intelligent wheelchair. *Transactions of the Institute of Measurement and Control*, doi: 10.1177/0142331215587041

Matveev, A.S., Teimoori, H., Savkin, A.V. (2011). Navigation of a unicycle-like mobile robot for environmental extremum seeking. *Automatica*, 47 (1), 85-91.

Utkin, V., Guldner J., Shi, J. (2009). *Sliding mode control in electromechanical systems*, CRC Press.

Vweza, A.O., Chong, K. T., Lee, D. J. (2015). Gradient-free numerical optimization-based extremum seeking control for multiagent systems. *International Journal of Control, Automation and Systems*, 13 (4), 877-886.

Zhang, C., Arnold, D., Ghods, N., Siranosian, A., Krstic, M. (2007). Source seeking with non-holonomic unicycle without position measurement and with tuning of forward velocity. *Systems and Control Letters*, 56, 245-252.

Zhang, C., Ordonez, R. (2007). Numerical optimization-based extremum seeking control with application to ABS design. *IEEE Transactions on Automatic Control*, 52 (3), 454-467.